

# The Method of Conditional Expectations for PAPR and Cubic Metric Reduction

Saeed Afrasiabi-Gorgani and Gerhard Wunder

## Abstract

The OFDM waveform exhibits high fluctuation in the signal envelope which causes distortion in the nonlinear power amplifier of the transmitter. Peak-to-Average Power Ratio (PAPR) and Cubic Metric (CM) are the common metrics to quantify the phenomenon. A promising approach for PAPR or CM reduction is Sign Selection which is based on altering the signs of the data symbols. In this paper, the Method of Conditional Expectations (CE Method) is proposed to obtain a competing suboptimal solution to the Sign Selection problem. For PAPR reduction, a surrogate metric is introduced which allows for an efficient application of the CE Method. For CM reduction, the tractability of the definition of CM is exploited to this end. The algorithm is analyzed to obtain an upper bound on the worst-case reduced metric value. A noticeable characteristic is the persistent reduction capability for a wide range of subcarrier numbers. In particular, simulations show a reduction of the so-called “effective PAPR” to about 6.5 dB from 10.5 dB and 11.7 dB respectively for 64 to 1024 subcarriers. A similar steady reduction of 3 dB is observed for CM. In addition, the CE Method leads to a pruned version of Sign Selection which halves the rate loss.

## Index Terms

Orthogonal Frequency Division Multiplexing (OFDM), Cubic Metric (CM), Peak-to-Average Power Ratio (PAPR)

## I. INTRODUCTION

Orthogonal Frequency Division Multiplexing (OFDM) is a well-known multicarrier waveform which has been used in the major wireless communication systems. A main drawback of OFDM

This work was supported by the German Research Foundation (DFG) grant WU 598/3-1.

The authors are with the Department of Mathematics and Computer Science, Freie Universität Berlin, 14195, Berlin, Germany, e-mail: s.afraziabi, g.wunder@fu-berlin.de.

scheme is the high dynamic range of its signal envelope, which causes nonlinear distortion at the output of the power amplifier [1]. In order to avoid the distortion, the so-called power back-off needs to be applied in the power amplifier. Consequently, the power amplifier operates with a low energy efficiency. Especially for mobile equipments where battery life is limited and power amplifiers cannot have a large linear range due to cost constraints, the problem is more pressing [2]. It is therefore critical to reduce the required power back-off.

The problem is commonly formulated as the minimization of a metric which captures the physical phenomenon and determines the power back-off. The classical metric is the ratio of the peak instantaneous signal power to the average power over consecutive signal segments referred to as Peak-to-Average-Power-Ratio (PAPR) [1]. An alternative metric called Cubic Metric (CM), which is based on the energy in the nonlinear distortion, was more recently proposed and reported to predict the required back-off more accurately [3].

The PAPR reduction problem has been tackled by several approaches, which can be broadly categorized into two groups. Methods based on deliberately introduced distortion constitute one category, with Clipping and Filtering [4] as a well-known example. The second category consists of the distortionless methods which typically provide PAPR reduction at the expense of some reserved resources which incurs rate loss, such as Selected Mapping (SLM) [5], Tone Reservation (TR) and Tone Injection (TI) [6]. The methods differ significantly at least in terms of reduction gain, rate loss, transmission power and complexity. A comparison of the pros and cons requires a separate study as provided, for instance, in [7]. A refreshed and fundamental review of the problem is as well provided in [8].

The CM reduction problem, on the other hand, has received limited attention compared to PAPR. In particular, very few of the already known methods from PAPR reduction research are examined for CM reduction, such as in [9], [10] and [11] for TR, Clipping and Filtering and SLM, respectively. It will be emphasized in this paper that CM has a more amenable mathematical structure, which indicates that there is room to improve on the performance and complexity of the back-off reduction problem by considering CM instead of PAPR, besides its reportedly higher accuracy.

Sign Selection is a promising distortionless approach based on altering the signs of the data symbols to reduce the PAPR, which has shown potentials for considerable reduction performance at the price of a rate loss equivalent to one bit per complex data symbol for each utilized sign variable [12–16]. Considering  $N$  subcarriers, there are  $2^N$  possible sign combinations, which

implies an exponential complexity order for the optimal sign selection. This has motivated research for competing suboptimal solutions. Some proposals with noticeable performance include the application of the method of Conditional Probabilities in [12], [13], a sign selection method guided by clipping noise in [14], a greedy algorithm in [15] and a cross-entropy-based algorithm in [16]. In this work, the method of Conditional Expectations (CE Method), originally proposed in fields of discrete mathematics and graph theory [17], is used to treat the Sign Selection problem to develop a simple algorithm with a competitive performance for both PAPR and CM reduction requiring only  $\frac{N}{2}$  sign bits.

The core idea of the CE method is to treat the optimization variables, i.e. the signs of the complex data symbols, as random variables. This artificial randomness is then employed to optimize the signs using conditional expectations. In addition to a direct application of the method to PAPR, a surrogate function referred to as Sum-Exp (SE) is proposed to gain indirect PAPR reduction. Unlike the other metrics, SE has no physical interpretation and is not directly related to power back-off. However, it will be shown that its reduction results in the reduction of the PAPR with lower complexity. The CE method is also applied to CM reduction, where the benefit of the mathematical tractability of CM in deriving low complexity closed-form expressions is demonstrated. As a rather uncommon characteristic among the solutions of the Sign Selection problem in the literature, an increasing reduction gain in PAPR and CM for increasing number of subcarriers is shown by simulations, which implies a roughly constant back-off for a large range of  $N$ . Furthermore, the CE method allows the analysis of the reduction performance by providing upper-bounds on reduced PAPR and CM values for any combination of the data symbols.

*Notation:* A random variable  $X$  is distinguished from a realization  $x$  by using upper and lower case letters, respectively. Vectors are shown by bold-face letters. For a vector  $\mathbf{x}$ , the notation  $x_{m:n}$  is the compact form for  $[x_m, x_{m+1}, \dots, x_n]$ . The expected value of  $Y$  with respect to the random variable  $X$  is denoted by  $\mathbb{E}_X[Y]$ , where the subscript may be omitted if clear from the context. Cardinality of a set  $\mathcal{S}$  is denoted by  $|\mathcal{S}|$ .

## II. PRELIMINARIES

In this section, the OFDM signal model as well as the definitions of the metrics PAPR, SE and CM are first presented. Then the Sign Selection problem is formalized and discussed.

### A. Signal Model

Consider an OFDM scheme with  $N$  subcarriers. Let  $\mathcal{M}$  be the set of the complex-valued constellation points. The data symbols that modulate the subcarriers are equiprobably and independently generated with zero mean, which implies that  $\sum_{x \in \mathcal{M}} x = 0$ . Accordingly, the random vector  $\mathbf{B} \in \mathcal{M}^N$  denotes the vector of data symbols in an OFDM symbol. Denoting the frequency separation of the first and the last subcarriers as  $F_s$ , the baseband continuous-time signal model for an OFDM symbol is

$$u(t, \mathbf{B}) = \frac{1}{\sigma_b \sqrt{N}} \sum_{k=0}^{N-1} B_k e^{i \frac{2\pi}{N} F_s k t} \quad t \in [0, T), \quad (1)$$

where  $T = \frac{N}{F_s}$  and the signal power is normalized by  $\sigma_b = \sqrt{\mathbb{E}[|u(t, \mathbf{B})|^2]}$ . With the sampling frequency  $LF_s$ , where  $L > 1$  is the oversampling factor, the discrete-time signal model for an OFDM symbol is

$$s(n, \mathbf{B}) = u\left(\frac{n}{LF_s}, \mathbf{B}\right) = \frac{1}{\sigma_b \sqrt{N}} \sum_{k=0}^{N-1} B_k e^{i \frac{2\pi}{LN} kn} \quad n = 0, 1, \dots, LN-1. \quad (2)$$

The oversampling is necessary for reliable measurement of PAPR and CM from the discrete-time signal [18], [19].

### B. Peak to Average Power Ratio (PAPR)

**Definition 1.** The PAPR metric is a function of the random data vector  $\mathbf{B} \in \mathcal{M}^N$  and is defined as

$$\theta_N(\mathbf{B}) = \max_{n=0,1,\dots,LN-1} |s(n, \mathbf{B})|^2, \quad (3)$$

where  $s(n, \mathbf{B})$  is given in (2) and  $L > 1$  is the oversampling factor.

It will be seen that the maximum operator in the definition of the PAPR makes the required derivations of the CE Method difficult. Here we propose the Sum-Exp (SE) metric, which will be shown to be a suitable objective function to replace PAPR such that a desirable indirect PAPR reduction is gained by SE reduction.

**Definition 2.** The SE metric is a function of the random data vector  $\mathbf{B} \in \mathcal{M}^N$  and is defined as

$$\zeta_N(\mathbf{B}) = \sum_{n=0}^{LN-1} e^{\kappa |s(n, \mathbf{B})|^2}, \quad (4)$$

where  $s(n, \mathbf{B})$  is given in (2),  $\kappa \geq 1$  is an adjustable parameter and  $L > 1$  is the oversampling factor.

The SE metric is obtained from the *log-sum-exp* function of the squared magnitude of the signal samples, i.e.  $\log \sum_{n=0}^{LN-1} e^{|s(n, \mathbf{B})|^2}$ , which is a well-known approximation of the maximum function [20] since

$$\max_{i=0, \dots, LN-1} |s(n, \mathbf{B})|^2 \leq \log \sum_{i=0}^{LN-1} e^{|s(n, \mathbf{B})|^2} \leq \max_{i=0, \dots, LN-1} |s(n, \mathbf{B})|^2 + \log LN.$$

The first inequality is strict unless  $LN = 1$  and approaches an equality as the maximum becomes larger relative to the rest of the samples, while the second inequality holds when all values are equal. That is, the approximation improves when the spread of the amplitudes of the signal samples is larger. Therefore, high ratio of the peak power to the average power of the OFDM signal implies that log-sum-exp is likely to be an acceptable approximation for PAPR. Furthermore, it motivates the introduction of the scaling factor  $\kappa \geq 1$  to modify the log-sum-exp function as  $\frac{1}{\kappa} \log \sum_{i=0}^{LN-1} e^{\kappa |s(n, \mathbf{B})|^2}$  to increase the spread. The SE metric is obtained from the modified log-sum-exp function by omitting the monotonically increasing log function as well as the constant  $\kappa^{-1}$ .

### C. Cubic Metric (CM)

CM [3] is based on the assumption of a third-order (cubic) polynomial model for the input-output relation of the power amplifier. That is, the output signal  $v_o(t)$  for a passband input signal  $v(t)$  is assumed to be

$$v_o(t) = g_1 v(t) + g_3 v^3(t), \quad t \in \mathbb{R},$$

where the linear gain  $g_1$  and the non-linear gain  $g_3$  are constant and related to the amplifier design. While PAPR is based only on the peaks of the instantaneous power, CM directly captures the energy in the distortion term  $v^3(t)$  and is calculated as

$$\text{CM}_{\text{dB}} = \frac{\text{RCM}_{\text{dB}}[v(t)] - \text{RCM}_{\text{dB}}[v_{\text{ref}}(t)]}{K_{\text{slp}}} + K_{\text{bw}},$$

where the subscript dB refers to the value in logarithmic scale and the Raw Cubic Metric (RCM) of a signal is defined as

$$\text{RCM}_{\text{dB}}[v(t)] = 20 \log_{10} \left( \text{rms} \left[ \left( \frac{v(t)}{\text{rms}[v(t)]} \right)^3 \right] \right). \quad (5)$$

The reference signal  $v_{\text{ref}}(t)$ , the slope factor  $K_{\text{slp}}$  and the bandwidth scaling factor  $K_{\text{bw}}$  [21] are independent of  $v(t)$  and are not discussed here. The Root Mean Square (RMS) of a signal  $v(t)$  over a large enough interval  $U \subset \mathbb{R}$  is  $\text{rms}[v(t)] = \sqrt{\frac{1}{U} \int_U v^2(t) dt}$ .

Consider that reduction of CM for  $v(t)$  is essentially equivalent to reduction of its RCM. In addition, CM and RCM are constants calculated for the whole continuous-time passband signal, whereas practical reduction algorithms operate over individual discrete-time baseband OFDM symbols. Therefore, the discrete-time baseband version of the RCM of an OFDM symbol is actually used for CM reduction, as done in [9–11], which is referred to as Symbol RCM (SRCM) in this paper.

**Definition 3.** SRCM is a function of the random data vector  $\mathbf{B} \in \mathcal{M}^N$  and is defined as

$$\eta_N(\mathbf{B}) = \frac{1}{LN} \sum_{n=0}^{LN-1} |s(n, \mathbf{B})|^6, \quad (6)$$

where  $s(n, \mathbf{B})$  is given in (2) and  $L > 1$  is the oversampling factor.

In order to show the relation of RCM and SRCM, we shall first briefly discuss the baseband representation of  $v^3(t)$ . Let the baseband equivalent representation of  $v(t)$  be  $h(t) = \sum_{m=-\infty}^{\infty} u(t - mT, \mathbf{B}_m)$  as a function of complex data symbols  $\mathbf{B}_m \in \mathcal{M}^N$  pertaining to consecutive OFDM symbols. By a suitable choice of the normalization factor, it follows from the standard procedure of passband to baseband conversion [22] that  $\text{rms}[v(t)] = \text{rms}[|h(t)|] = 1$ . Ignoring the scaling factors, it can as well be shown that  $h^*(t)|h(t)|^2$  is the baseband representation of the frequency component of  $v^3(t)$  at the carrier frequency [22], where  $h^*(t)$  is the complex conjugate of  $h(t)$ . Consequently,  $\text{RCM}[v(t)] = (\text{rms}[v^3(t)])^2 = A (\text{rms}[|h(t)|^3])^2$  for some scalar  $A$  gives the RCM in terms of the baseband continuous signal. Next, the discrete-time version of  $h(t)$  is  $h(n) = \sum_{m=-\infty}^{\infty} s(n - mLN, \mathbf{B}_m)$ . Replacing the summation with an integral in calculation of the RMS of a discrete-time signal, we have  $\text{rms}[|h(t)|^3] \simeq \text{rms}[|h(n)|^3]$  given adequate oversampling. Finally, RCM can be written as

$$\begin{aligned} \text{RCM}[v(t)] &\simeq \lim_{K \rightarrow \infty} \frac{1}{K} \sum_{n=0}^K |h(n)|^6 \\ &= \lim_{M \rightarrow \infty} \frac{1}{2MLN} \sum_{m=-M}^{M-1} \sum_{n=0}^{LN-1} |s(n - mLN, \mathbf{B}_m)|^6 \\ &= \lim_{M \rightarrow \infty} \frac{1}{2M} \sum_{m=-M}^{M-1} \eta_N(\mathbf{B}_m). \end{aligned} \quad (7)$$

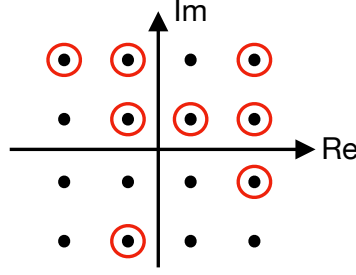


Fig. 1: A non-unique choice of  $\mathcal{C}$  from  $\mathcal{M}$  for the 16-QAM constellation.

Therefore, RCM of the OFDM signal is the average of the SRCM values of the underlying OFDM symbols.

#### D. The Sign Selection Problem

As introduced before, Sign Selection refers to altering the signs of the data symbols in an OFDM symbol in order to reduce a desired metric, such as PAPR and CM. Therefore, for the constellation  $\mathcal{M}$ ,  $\log_2 |\mathcal{M}| - 1$  bits per transmitted data symbol carry information and one bit is determined by the adopted Sign Selection algorithm. To perform the bit-to-symbol mapping in the transmitter, initially consider taking independently and equiprobably distributed random sign bits to complete the  $\log_2 |\mathcal{M}|$ -bit blocks. This formulation helps analytical derivations in later sections and will be shortly shown not to affect the solution. For the resulting vector of complex data symbols  $\mathbf{b} \in \mathcal{M}^N$ , the Sign Selection approach seeks a solution  $\mathbf{x}^*$  for the problem

$$\min_{\mathbf{x} \in \{-1, 1\}^N} f(\mathbf{b} \odot \mathbf{x}), \quad (8)$$

where  $f(\cdot) \geq 0$  is a metric defined on the OFDM symbol and  $\odot$  denotes element-wise multiplication of vectors. Accordingly,  $\mathbf{b} \odot \mathbf{x}^*$  will be the transmitted symbols. Considering that the solution space of (8) grows exponentially with  $N$ , the objective of this paper is to derive an efficient algorithm to obtain a suboptimal solution.

Now we justify that the random sign bits used to complete the  $\log_2 |\mathcal{M}|$ -bit blocks do not alter the minimization problem. Assume that the constellation  $\mathcal{M}$  is symmetric such that for each point  $y \in \mathcal{M}$ , the negated value  $-y$  is in the set. Let  $\mathcal{C} \subset \mathcal{M}$  be a non-unique choice of  $\frac{|\mathcal{M}|}{2}$  points of  $\mathcal{M}$  such that if  $y \in \mathcal{C}$ , then  $-y \notin \mathcal{C}$ . A sample choice of  $\mathcal{C}$  for 16-QAM is shown

in Fig. 1. For every  $\mathbf{c} \in \mathcal{C}^N$ , let  $\Omega_{\mathbf{c}} = \{\mathbf{c} \odot \mathbf{x}, \mathbf{x} \in \{-1, 1\}^N\}$ . The space of the data vectors  $\mathcal{M}^N$  can be partitioned into the sets  $\Omega_{\mathbf{c}}$  for  $\mathbf{c} \in \mathcal{C}^N$  such that

$$\mathcal{M}^N = \bigcup_{\mathbf{c} \in \mathcal{C}^N} \Omega_{\mathbf{c}} \quad (9)$$

and  $\Omega_{\mathbf{c}} \cap \Omega_{\mathbf{c}'} = \emptyset$  when  $\mathbf{c} \neq \mathbf{c}'$ . Therefore, every  $\mathbf{b}$  in (8) belongs to a partition  $\Omega_{\mathbf{d}}$  such that  $\mathbf{d} \in \mathcal{C}^N$  and  $\mathbf{b} = \mathbf{d} \odot \mathbf{v}$  for some  $\mathbf{v} \in \{-1, 1\}^N$ . Having all possible sign vectors as the solution space, it is clear that the Sign Selection problem always seeks the minimum of the partition which contains  $\mathbf{b}$ . Formally,  $\min_{\mathbf{x} \in \{-1, 1\}^N} f(\mathbf{b} \odot \mathbf{x}) = \min_{\mathbf{x} \in \Omega_{\mathbf{d}}} f(\mathbf{x})$  for every  $\mathbf{b} \in \Omega_{\mathbf{d}}$ . Notice that although the starting vector  $\mathbf{b} \in \Omega_{\mathbf{d}}$  does not affect the solution of (8) for the partition  $\Omega_{\mathbf{d}}$ , it may change the suboptimal solution provided by a proposed algorithm.

The (bit-to-)symbol mapping in the transmitter and the decoding in the receiver are based on a predetermined  $\mathcal{C}$ . On the transmitter side, the data symbols are obtained by mapping  $\log_2 |\mathcal{M}| - 1$  bits to a point in  $\mathcal{C}$ . On the receiver side, the decoding of the symbol of each subcarrier is performed by choosing  $c \in \mathcal{C}$  when one of  $\pm c \in \mathcal{M}$  is detected and reversing the symbol mapping accordingly. Notice that the decoding adds no complexity to the receiver. Besides, the choice of  $\mathcal{C}$  plays a role only in the symbol mapping and decoding and is otherwise immaterial to the Sign Selection problem. Particularly, it can be shown that the partitioning described before is independent of  $\mathcal{C}$ .

As the final comment, sign selection clearly incurs rate loss. Consider the generalized scheme where  $N_s \leq N$  signs are used in the sign selection. That is,  $N_s$  data symbols carry  $\log_2 |\mathcal{M}| - 1$  bits of information and the remaining  $N - N_s$  data symbols are mapped from  $\log_2 |\mathcal{M}|$  bits to  $\mathcal{M}$ . The incurred amount of rate loss, i.e. the ratio of the bits used for Sign Selection to the total number of bits in an OFDM symbol, is

$$R = \frac{N_s}{N \log_2 |\mathcal{M}|} = \frac{N_s}{N} \log_{|\mathcal{M}|} 2. \quad (10)$$

Evidently, the rate loss is inversely proportional to the constellation size  $|\mathcal{M}|$ .

### III. METHOD OF CONDITIONAL EXPECTATIONS

The CE Method [17] is represented here for obtaining a suboptimal solution to the Sign Selection problem for reduction of an arbitrary metric  $f(\cdot) \geq 0$ . For a given data vector  $\mathbf{b} \in \mathcal{M}^N$ , a random vector of sign variables  $\mathbf{X} \in \{-1, 1\}^N$  is initially assumed with equiprobable and independent elements, which are then sequentially decided and fixed. Consider the  $j^{\text{th}}$  iteration



where the random signs  $X_{0:j-1}$  are fixed to  $x_{0:j-1}^*$ . The expected values of  $f(\mathbf{b} \odot \mathbf{X})$  conditioned on  $X_{0:j-1} = x_{0:j-1}^*$  with  $X_j = 1$  and  $X_j = -1$  are compared and the sign that yields the smaller expectation is chosen as  $x_j^*$ . Formally, a sub-optimal solution to the minimization problem stated in (8) can be obtained by sequentially choosing the sign variables as

$$x_j^* = \begin{cases} \arg \min_{x_0 \in \{\pm 1\}} \mathbb{E}[f(\mathbf{b} \odot \mathbf{X}) | X_0 = x_0] & j = 0 \\ \arg \min_{x_j \in \{\pm 1\}} \mathbb{E}[f(\mathbf{b} \odot \mathbf{X}) | X_{0:j-1} = x_{0:j-1}^*, X_j = x_j] & j = 1, \dots, N-1. \end{cases} \quad (11)$$

The decision rule given in (11) is based on introducing random sign variables and then reducing the conditional expectation of the original objective function. The justification that (11) leads to a desirable suboptimal solution of (8) is explained partly here for the general metric  $f$  and will be concluded in Section V for PAPR and SRCM. For the  $j^{\text{th}}$  sign decision, let

$$g_j^\pm(\mathbf{b}) = \begin{cases} \mathbb{E}[f(\mathbf{b} \odot \mathbf{X}) | X_0 = \pm 1] & j = 0 \\ \mathbb{E}[f(\mathbf{b} \odot \mathbf{X}) | X_{0:j-1} = x_{0:j-1}^*, X_j = \pm 1] & j = 1 \dots, N-1. \end{cases} \quad (12)$$

Following the decision criterion in (11), we have

$$\mathbb{E}[f(\mathbf{b} \odot \mathbf{X}) | X_{0:j} = x_{0:j}^*] = \min \{g_j^+(\mathbf{b}), g_j^-(\mathbf{b})\},$$

whereas for the  $(j-1)$ -th step with  $j \geq 1$ , it holds that

$$\begin{aligned} \mathbb{E}[f(\mathbf{b} \odot \mathbf{X}) | X_{0:j-1} = x_{0:j-1}^*] &= g_j^+(\mathbf{b})\mathbb{P}(X_j = 1 | X_{0:j-1} = x_{0:j-1}^*) \\ &\quad + g_j^-(\mathbf{b})\mathbb{P}(X_j = -1 | X_{0:j-1} = x_{0:j-1}^*) \\ &= g_j^+(\mathbf{b})\mathbb{P}(X_j = 1) + g_j^-(\mathbf{b})\mathbb{P}(X_j = -1) \\ &= \frac{1}{2}(g_j^+(\mathbf{b}) + g_j^-(\mathbf{b})) \\ &\geq \min\{g_j^+(\mathbf{b}), g_j^-(\mathbf{b})\}. \end{aligned}$$

Therefore,

$$\mathbb{E}[f(\mathbf{b} \odot \mathbf{X}) | X_{0:j} = x_{0:j}^*] \leq \mathbb{E}[f(\mathbf{b} \odot \mathbf{X}) | X_{0:j-1} = x_{0:j-1}^*]$$

for  $j = 1, \dots, N-1$ . This shows that for a given  $\mathbf{b}$ , the non-increasing sequence of the conditional expectations begins with the *initial expectation*  $\mathbb{E}_{\mathbf{X}}[f(\mathbf{b} \odot \mathbf{X})]$  and ends with  $f(\mathbf{b} \odot \mathbf{x}^*) = \mathbb{E}[f(\mathbf{b} \odot \mathbf{X}) | \mathbf{X} = \mathbf{x}^*]$  where no randomness is left. That is, the last conditional expectation coincides with a metric value such that

$$f(\mathbf{b} \odot \mathbf{x}^*) \leq \mathbb{E}_{\mathbf{X}}[f(\mathbf{b} \odot \mathbf{X})]. \quad (13)$$

This justifies that the decision criterion given in (11) leads to a value of the original metric  $f$  with the property stated above. Proving the reduction and the upper-bound on the reduced values is not known for the general case of the arbitrary metric  $f$  and will be treated in Section V specifically for PAPR and CM. Calculation of the conditional expectations required at each step is a major step in development of the algorithm and will be discussed in Section IV.

#### IV. CALCULATION OF THE CONDITIONAL EXPECTATIONS

For a given vector of data symbols  $\mathbf{b}$ , the decision for  $x_j^*$  requires calculation of  $g_j^\pm(\mathbf{b})$  in (12) which is compactly rewritten as

$$g_j^\pm(\mathbf{b}) = \mathbb{E}[f(\mathbf{b} \odot \mathbf{Y}_j^\pm)], \quad (14)$$

where

$$\mathbf{Y}_j^\pm = [x_0^*, x_1^*, \dots, x_{j-1}^*, \pm 1, X_{j+1}, \dots, X_{N-1}]^T$$

encapsulates the decided signs, the new sign variable set to  $+1$  or  $-1$  and the remaining random sign variables. The obvious way of calculating the conditional expectations for practically any metric  $f$  is to use the empirical average  $\hat{g}_j^\pm(\mathbf{b}, \mathbf{X}^{1:Q})$  to estimate  $g_j^\pm(\mathbf{b})$ , which is

$$\hat{g}_j^\pm(\mathbf{b}, \mathbf{X}^{1:Q}) = \frac{1}{Q} \sum_{l=1}^Q f(\mathbf{b} \odot \psi_j^\pm(\mathbf{X}^l)), \quad (15)$$

where  $Q$  is the number of realizations of the random sign vector used for the estimation and

$$\psi_j^\pm(\mathbf{X}^l) = [x_0^*, \dots, x_{j-1}^*, \pm 1, X_0^l, \dots, X_{N-j-2}^l]^T, \quad (16)$$

where the random variables  $X_k^l \in \{-1, 1\}$ ,  $l = 1, 2, \dots, Q$ ,  $k = 0, 1, \dots, N - j - 2$  are independent and equiprobable.

Deriving more efficient ways of calculating the conditional expectations  $g_j^\pm(\mathbf{b})$  is a pivotal part of the proposed method. The PAPR metric does not lend itself well to mathematical manipulations to obtain closed-form expressions. Consequently, the conditional expectations are estimated by the sample average as in (15), which will be further discussed. On the contrary, the definitions of SRCM and SE together with the statistical properties of the signal samples  $s(n, \mathbf{b} \odot \mathbf{Y}_j^\pm)$  make it possible to derive closed-form expressions for  $g_j^\pm(\mathbf{b})$ . These results depend on convergence of the signal samples in distribution to a Gaussian random variable, proof of which is not trivial due to the specific signal model imposed by the Sign Selection problem. This will be clarified in the second part of this section before treating the calculations for SE and SRCM.

### A. PAPR metric

As mentioned before, the available method for calculation of the conditional expectations of PAPR is to perform estimation as specified in (15). It is apt to study the estimator in terms of a relation between the amount of the required numerical computations, which is proportional to  $Q$ , and the performance. Although such analysis for PAPR was not reached, authors have presented interesting results in [23] for the closely related metric

$$\phi_N(\mathbf{b}) = \sqrt{\theta_N(\mathbf{b})}, \quad (17)$$

which is referred to as Crest Factor (CF). This is a valid alternative as firstly CF has the same physical meaning and practical significance and secondly its relation with PAPR is monotonically increasing. In addition, simulations show almost identical PAPR reduction gained by reduction of CF.

Accordingly, consider  $g_j^\pm(\mathbf{b})$  in (14) for  $f(\mathbf{b} \odot \mathbf{Y}_j^\pm) = \phi_N(\mathbf{b} \odot \mathbf{Y}_j^\pm)$ . The sample average with  $Q$  realizations of the sign vector is

$$\hat{g}_j^\pm(\mathbf{b}, \mathbf{X}^{1:Q}) = \frac{1}{Q} \sum_{l=1}^Q \phi_N(\mathbf{b} \odot \psi_j^\pm(\mathbf{X}^l)), \quad (18)$$

where  $\psi_j^\pm(\mathbf{X}^l)$  and the random vectors  $\mathbf{X}^l, l = 1, 2, \dots, Q$  were defined in (16). It is clear that  $\mathbb{E}[\hat{g}_j^\pm(\mathbf{b}, \mathbf{X}^{1:Q})] = g_j^\pm(\mathbf{b})$ . Consequently,  $\lim_{Q \rightarrow \infty} \hat{g}_j^\pm(\mathbf{b}, \mathbf{X}^{1:Q}) = g_j^\pm(\mathbf{b})$  as the variance of  $\theta_N(\mathbf{b} \odot \psi_j^\pm(\mathbf{X}^l))$  is finite. In order to obtain a relation between the reliability of the estimation and  $Q$ , McDiarmid's concentration inequality [24] was employed to bound the probability of deviation of the estimate from its true value as stated in the following theorem [23]. The proof is provided in Appendix A for completeness.

**Theorem 1.** *Consider the sample average  $\hat{g}_j^\pm(\mathbf{b}, \mathbf{X}^{1:Q})$  given in (18) as an estimate of the conditional expectation  $g_j^\pm(\mathbf{b})$  given in (14) with  $f(\mathbf{b} \odot \mathbf{Y}_j^\pm) = \phi_N(\mathbf{b} \odot \mathbf{Y}_j^\pm)$ . For any  $\mathbf{b} \in \mathcal{M}^N$  and  $\epsilon \geq 0$ ,*

$$\mathbb{P}(|\hat{g}_j^\pm(\mathbf{b}, \mathbf{X}^{1:Q}) - g_j^\pm(\mathbf{b})| \geq \epsilon) \leq 2 \exp\left(-2\epsilon^2 \frac{Q}{d^2 (N - j - 1)}\right),$$

where  $d = 2\sigma_b^{-1} \max_{x \in \mathcal{M}} |x|$ .

An interesting result of Theorem 1 is that the upperbound on the probability of deviation is independent of  $N$ . This is further clarified as follows. A lower bound on the required  $Q$  which

guarantees the probability of deviation by  $\epsilon$  from the true value to be less than  $p$  can be deduced within the context of Theorem 1 as

$$Q_o = -\frac{d^2 \log \frac{p}{2}}{2\epsilon^2} \frac{N - j - 1}{N}.$$

In particular, it indicates that  $Q_o$  is proportional to the ratio of the number of the remaining sign variables to the total number of them. Equivalently,

$$Q_o \approx -\frac{d^2 \log \frac{p}{2}}{2\epsilon^2} (1 - \rho), \quad (19)$$

where  $\rho = \frac{j}{N}$  and the approximation is due to  $\frac{N-1}{N} \approx 1$  for large  $N$ . However, establishing a connection between the probability of error in sign decision and  $Q$  is challenging and needs further research.

### B. Distribution of $s(n, \mathbf{b} \odot \mathbf{Y}_j^\pm)$

We begin with characterizing the distribution of the continuous-time OFDM symbol  $u(t, \mathbf{b} \odot \mathbf{Y}_j^\pm)$  in Theorem 2, which is required for performance analysis in Section V. The distribution of the discrete-time version  $s(n, \mathbf{b} \odot \mathbf{Y}_j^\pm)$  follows automatically, as stated in Corollary 1, which is used in the derivation of the conditional expectations of SRCM and SE. As the first step, the following Lemma gives the covariance functions of the samples of the OFDM signal for a given  $\mathbf{b}$  and iteration  $j$  of the CE Method as  $N \rightarrow \infty$ . Let

$$\begin{aligned} \hat{u}_r(t, \mathbf{b} \odot \mathbf{Y}_j^\pm) &= u_r(t, \mathbf{b} \odot \mathbf{Y}_j^\pm) - \mathbb{E}[u_r(t, \mathbf{b} \odot \mathbf{Y}_j^\pm)], \\ \hat{u}_i(t, \mathbf{b} \odot \mathbf{Y}_j^\pm) &= u_i(t, \mathbf{b} \odot \mathbf{Y}_j^\pm) - \mathbb{E}[u_i(t, \mathbf{b} \odot \mathbf{Y}_j^\pm)], \end{aligned} \quad (20)$$

where subscripts  $r$  and  $i$  denote the real and imaginary parts respectively.

**Lemma 1.** *Consider  $j = \rho N$  where  $0 \leq \rho \leq 1$  is a rational number. For  $\mathbf{B}$  randomly distributed in  $\mathcal{M}^N$ , let the variances and covariances of  $u_r(t, \mathbf{B} \odot \mathbf{Y}_j^\pm)$  and  $u_i(t, \mathbf{B} \odot \mathbf{Y}_j^\pm)$  with respect to  $\mathbf{Y}_j^\pm$  as  $N \rightarrow \infty$  and at any time instances  $t_1, t_2 \in [0, T)$  be denoted as*

$$\begin{aligned} R_{rr}^j(\tau, \mathbf{B}) &= \lim_{N \rightarrow \infty} \mathbb{E}_{\mathbf{Y}_j^\pm} [\hat{u}_r(t_1, \mathbf{B} \odot \mathbf{Y}_j^\pm) \hat{u}_r(t_2, \mathbf{B} \odot \mathbf{Y}_j^\pm)], \\ R_{ri}^j(\tau, \mathbf{B}) &= \lim_{N \rightarrow \infty} \mathbb{E}_{\mathbf{Y}_j^\pm} [\hat{u}_r(t_1, \mathbf{B} \odot \mathbf{Y}_j^\pm) \hat{u}_i(t_2, \mathbf{B} \odot \mathbf{Y}_j^\pm)], \\ R_{ii}^j(\tau, \mathbf{B}) &= \lim_{N \rightarrow \infty} \mathbb{E}_{\mathbf{Y}_j^\pm} [\hat{u}_i(t_1, \mathbf{B} \odot \mathbf{Y}_j^\pm) \hat{u}_i(t_2, \mathbf{B} \odot \mathbf{Y}_j^\pm)], \end{aligned}$$

where  $\tau = t_2 - t_1 \in (-T, T)$ . Then

$$R_{rr}^j(\tau) = R_{ii}^j(\tau) = \frac{\sigma_b^2}{2}(\text{sinc}(2F_s\tau) - \rho\text{sinc}(2F_s\tau\rho)),$$

$$R_{ri}^j(\tau) = \begin{cases} \frac{\sigma_b^2}{2} \frac{1}{2\pi F_s \tau} \left( \frac{1}{\rho} \cos(2\pi F_s \rho \tau) - \cos(2\pi F_s \tau) \right) & \tau \neq 0 \\ 0 & \tau = 0 \end{cases},$$

with probability one. That is, the result holds for any  $\mathbf{B}$  as  $N \rightarrow \infty$  which is emphasized by omitting the argument  $\mathbf{B}$  from the notation. Clearly,  $R_{ri}^j(\tau) = R_{ir}^j(-\tau)$ .

The proof is given in Appendix B. The following theorem characterizes the distribution of the OFDM signal.

**Theorem 2.** For  $\mathbf{B}$  randomly distributed in  $\mathcal{M}^N$  and  $j = \rho N$  as specified in Lemma 1, consider  $\hat{u}(t, \mathbf{B} \odot \mathbf{Y}_j^\pm)$  as defined in (20) at any set of time instances  $\{t_1, t_2, \dots, t_K\} \in [0, T)^K, K > 1$ . Omitting  $\mathbf{B} \odot \mathbf{Y}_j^\pm$  to save space, the vector

$$[\hat{u}_r(t_1), \hat{u}_i(t_1), \hat{u}_r(t_2), \hat{u}_i(t_2), \dots, \hat{u}_r(t_K), \hat{u}_i(t_K)]^T \quad (21)$$

converges in distribution, as  $N \rightarrow \infty$ , to the vector

$$[x_1, y_1, x_2, y_2, \dots, x_K, y_K]^T \quad (22)$$

of jointly Gaussian random variables with  $\mathbb{E}[x_m x_n] = R_{rr}^j(t_n - t_m)$ ,  $\mathbb{E}[y_m y_n] = R_{ii}^j(t_n - t_m)$  and  $\mathbb{E}[x_m y_n] = R_{ri}^j(t_n - t_m)$  as given in Lemma 1.

*Proof.* The proof follows a standard procedure and is only outlined here. It essentially consists of the application of the Cramer-Wold theorem [25] to the vector in (21) which requires that every linear combination of the elements of the vector in (21) converges in distribution to the same linear combination of the corresponding elements of the vector in (22). This can be verified by the Lindeberg condition. In this procedure, the existence of the covariances of the linear combination is shown in Lemma 1.  $\square$

From Theorem 2, the following result is immediate for the discrete-time OFDM signal at iteration  $j$ .

**Corollary 1.** For any given  $\mathbf{b} \in \mathcal{M}^N$ ,  $n = 0, 1, \dots, LN - 1$  and  $j = \rho N$  as defined in Lemma 1, it holds that

$$\begin{bmatrix} s_r(n, \mathbf{b} \odot \mathbf{Y}_j^\pm) - \mu_r(n, \mathbf{b} \odot \mathbf{Y}_j^\pm) \\ s_i(n, \mathbf{b} \odot \mathbf{Y}_j^\pm) - \mu_i(n, \mathbf{b} \odot \mathbf{Y}_j^\pm) \end{bmatrix} \xrightarrow{d} \mathcal{N}(0, \frac{1}{2}(1 - \rho)I),$$

where  $\xrightarrow{d}$  denotes convergence in distribution,  $I$  is a  $2 \times 2$  identity matrix and

$$\begin{aligned}\mu_r(n, \mathbf{b} \odot \mathbf{Y}_j^\pm) &= \frac{1}{\sigma_b \sqrt{N}} \operatorname{Re} \left\{ \pm b_j e^{i \frac{2\pi}{LN} j n} + \sum_{k=0}^{j-1} b_k x_k^* e^{i \frac{2\pi}{LN} k n} \right\}, \\ \mu_i(n, \mathbf{b} \odot \mathbf{Y}_j^\pm) &= \frac{1}{\sigma_b \sqrt{N}} \operatorname{Im} \left\{ \pm b_j e^{i \frac{2\pi}{LN} j n} + \sum_{k=0}^{j-1} b_k x_k^* e^{i \frac{2\pi}{LN} k n} \right\}.\end{aligned}$$

**Remark 1.** A pivotal result which enables the analytical derivations in the remainder of this paper is that at every iteration of the algorithm, the distribution of  $\hat{u}(t, \mathbf{b} \odot \mathbf{Y}_j^\pm)$  in the limit is independent of  $\mathbf{b}$ . In addition, the distribution of  $u(t, \mathbf{b} \odot \mathbf{X})$ , i.e. prior to any sign decision, is identical to that of  $u(t, \mathbf{B})$  as  $N \rightarrow \infty$ .

**Remark 2.** In the following sections, the asymptotically Gaussian distribution shown in Corollary 1 is used to approximate the distribution of  $s(n, \mathbf{b} \odot \mathbf{Y}_j^\pm)$  for the finite but large enough number of random sign variables, i.e.  $N - j - 1$  at iteration  $j$ . This can be used to derive closed-form expressions of the sign decision criterion (11) only for  $j = 0, 1, \dots, N - N_e - 1$ . The number of the excluded signs  $N_e$ , for which the approximation is unacceptable, will be determined based on simulations in Section VI.

### C. SE Metric

By substituting  $\zeta_N(\mathbf{b} \odot \mathbf{Y}_j^\pm)$  for  $f(\mathbf{b} \odot \mathbf{Y}_j^\pm)$  in (14), we have

$$g_j^\pm(\mathbf{b}) = \sum_{n=0}^{LN-1} \mathbb{E} \left[ e^{\kappa |s(n, \mathbf{b} \odot \mathbf{Y}_j^\pm)|^2} \right]. \quad (23)$$

It was shown in Corollary 1 that the real and imaginary components of  $s(n, \mathbf{b} \odot \mathbf{Y}_j^\pm)$  are Gaussian and independent in the limit with equal variances. For  $j = \rho N$ , let  $\delta_j^2 = R_{rr}(0) = R_{ii}(0) = \frac{1}{2}(1 - \rho)$  as obtained in Lemma 1. Here we apply the approximation suggested in Remark 2 for  $j = 0, \dots, N - N_e - 1$ . Specifically, the real and imaginary parts of

$$z(n, \mathbf{b} \odot \mathbf{Y}_j^\pm) = \delta_j^{-1} s(n, \mathbf{b} \odot \mathbf{Y}_j^\pm), \quad j = 0, \dots, N - N_e - 1 \quad (24)$$

have approximately unit variances with accordingly scaled expected values. Therefore,  $|z(n, \mathbf{b} \odot \mathbf{Y}_j^\pm)|^2$  for large enough  $N - j$  is approximately a non-central  $\chi^2$ -distributed random variable with two degrees of freedom. Consider the moment generating function of  $|z(n, \mathbf{b} \odot \mathbf{Y}_j^\pm)|^2$  which is

$$\begin{aligned}M_{j,n}^\pm(t) &= \mathbb{E} \left[ e^{t |z(n, \mathbf{b} \odot \mathbf{Y}_j^\pm)|^2} \right] \\ &= e^{\lambda_{j,n}^\pm t (1-2t)^{-1}} (1-2t)^{-1} \quad 2t < 1,\end{aligned}$$

where the non-centrality parameter  $\lambda_{j,n}^\pm$  is

$$\lambda_{j,n}^\pm = \delta_j^{-2} (\mu_r^2(n, \mathbf{b} \odot \mathbf{Y}_j^\pm) + \mu_i^2(n, \mathbf{b} \odot \mathbf{Y}_j^\pm)),$$

and  $\mu_r$  and  $\mu_i$  were given in Corollary 1. It can be seen that the terms in (23) are identical to the definition of  $M_{j,n}^\pm(\kappa\delta_j^2)$ . Consequently,

$$g_j^\pm(\mathbf{b}) = (\kappa\delta_j^2)^{-1} \beta \sum_{n=0}^{LN-1} e^{\beta\lambda_{j,n}^\pm}, \quad j = 0, \dots, N - N_e - 1, \quad (25)$$

where  $\beta = \kappa\delta_j^2(1 - 2\kappa\delta_j^2)^{-1}$ . Finally, a closed-form decision rule can be obtained as

$$x_j^* = -\text{sign} \left[ \sum_{n=0}^{LN-1} (e^{\beta\lambda_{j,n}^+} - e^{\beta\lambda_{j,n}^-}) \right], \quad j = 0, \dots, N - N_e - 1. \quad (26)$$

The number of the last sign decisions which do not follow the closed-form expression in (25), i.e.  $N_e$ , will be determined in Section VI. A sample average must be inevitably used instead for signs  $j = N - N_e, \dots, N - 1$  as in (15).

#### D. Cubic Metric

Replacing  $f(\mathbf{b} \odot \mathbf{Y}_j^\pm)$  with  $\eta_N(\mathbf{b} \odot \mathbf{Y}_j^\pm)$  in (14), we have [26]

$$g_j^\pm(\mathbf{b}) = \frac{1}{LN} \sum_{n=0}^{LN-1} \mathbb{E} \left[ |s(n, \mathbf{b} \odot \mathbf{Y}_j^\pm)|^6 \right]. \quad (27)$$

The expected values are the third moments of  $|s(n, \mathbf{b} \odot \mathbf{Y}_j^\pm)|^2$ . Following the approximation mentioned in Remark 2, they can be obtained from the third derivative of the moment generating function of the  $\chi^2$  random variable  $|z(n, \mathbf{b} \odot \mathbf{Y}_j^\pm)|^2$  as defined in (24). That is,

$$\mathbb{E} \left[ |s(n, \mathbf{b} \odot \mathbf{Y}_j^\pm)|^6 \right] = \delta_j^6 \frac{d^3 M_{j,n}^\pm(t)}{dt^3} \Big|_{t=0}, \quad j = 0, \dots, N - N_e - 1.$$

Obtaining the derivative and substituting it in (27), we have [26]

$$g_j^\pm(\mathbf{b}) = \frac{\sigma^6}{LN} \sum_{n=0}^{LN-1} [(\lambda_{j,n}^\pm)^3 + 18(\lambda_{j,n}^\pm)^2 + 72\lambda_{j,n}^\pm + 48], \quad j = 0, \dots, N - N_e - 1,$$

and the decision rule in (11) can be written in closed form as

$$x_j^* = -\text{sign} \left( \sum_{n=0}^{LN-1} [(\lambda_{j,n}^+)^3 + 18(\lambda_{j,n}^+)^2 + 72\lambda_{j,n}^+ - (\lambda_{j,n}^-)^3 - 18(\lambda_{j,n}^-)^2 - 72\lambda_{j,n}^-] \right) \quad (28)$$

for  $j = 0, \dots, N - N_e - 1$ . For the sign variables  $j = N - N_e, \dots, N - 1$ , consider using sample averages as in (15) with a high  $Q$ , which was the number of realizations of the random sign variables to calculate the conditional expectations. Simulations have shown that the CE Method

---

**Algorithm 1** Implementation of the CE Method for CM reduction by Sign Selection.

---

**Input:**  $b_0, \dots, b_{N_f-1}$ : data symbols with  $\log_2 |\mathcal{M}|$ -bit mapping

$b_{N_f}, \dots, b_{N-1}$ : data symbols with  $(\log_2 |\mathcal{M}| - 1)$ -bit mapping

```

1:  $\mathbf{x}^* \leftarrow [1, 1, \dots, 1]_{N \times 1}$ 
2:  $\mathbf{n} \leftarrow [0, 1, 2, \dots, LN - 1]$ 
3:  $\mathbf{h} \leftarrow \sum_{j=0}^{N_f-1} b_j \exp(i2\pi j \frac{\mathbf{n}}{LN})$ 
   {Element-wise operations on arrays are assumed in this pseudocode.}
4: for  $j = N_f$  to  $N - 1$  do
5:    $\mathbf{p} \leftarrow \mathbf{h} + b_j \exp(i2\pi j \frac{\mathbf{n}}{LN})$ 
6:    $\mathbf{m} \leftarrow \mathbf{h} - b_j \exp(i2\pi j \frac{\mathbf{n}}{LN})$ 
7:    $x_j^* \leftarrow -\text{sign}(\text{sum}(|\mathbf{p}|^6 + 18|\mathbf{p}|^4 + 72|\mathbf{p}|^2 - |\mathbf{m}|^6 - 18|\mathbf{m}|^4 - 72|\mathbf{m}|^2))$ 
8:   if  $x_j^* = 1$  then
9:      $\mathbf{h} \leftarrow \mathbf{p}$ 
10:  else
11:     $\mathbf{h} \leftarrow \mathbf{m}$ 
12:  end if
13: end for
14: return  $\mathbf{x}^*$ 

```

---

delivers the same performance for several nonzero values of  $N_e$  as for  $N_e = 0$ . That is, using accurate sample averages for the final sign variables does not improve the performance.

The application of the CE Method to the Sign Selection problem essentially leads to the explicit sign decision criteria derived in this section for PAPR and its substitute SE as well as for the SRCM. For better readability, the pseudocode for SRCM reduction is shown in Algorithm 1, where the expected values required for obtaining  $\lambda_{j,n}^\pm$  are constructed by adding the contribution of one subcarrier at each iteration (see lines 5 and 6).

## V. PERFORMANCE ANALYSIS

The CE Method guarantees (13), which is rewritten here for convenience:

$$f(\mathbf{b} \odot \mathbf{x}^*) \leq \mathbb{E}[f(\mathbf{b} \odot \mathbf{X})],$$



for a given  $\mathbf{b}$ . In order to characterize  $f(\mathbf{b} \odot \mathbf{x}^*)$ , one approach can be to establish a relation between the distribution of the initial expectation  $\mathbb{E}_{\mathbf{X}}[f(\mathbf{B} \odot \mathbf{X})]$  and that of the uncoded metric values  $f(\mathbf{B})$ ,  $\mathbf{B} \in \mathcal{M}^N$ . The analysis will be done for PAPR and SRCM with the help of some useful results from the literature. Concerning the SE metric, a relevant analysis would include a relation between SE reduction and the resulting indirect PAPR reduction, which requires further research.

#### A. PAPR metric

**Theorem 3.** *For any  $\mathbf{b} \in \mathcal{M}^N$ , the reduced PAPR value  $\theta_N(\mathbf{b} \odot \mathbf{x}^*)$  obtained by the CE Method is bounded in the limit as*

$$\lim_{N \rightarrow \infty} \frac{\theta_N(\mathbf{b} \odot \mathbf{x}^*) - a_N}{b_N} \leq \gamma,$$

where  $b_N = \frac{1}{2}$ ,  $a_N = 2 \log N + \log \log N + \log \frac{\pi}{3}$  and  $\gamma \approx 0.577$  is the Euler constant.

*Proof.* Consider the PAPR of the continuous-time OFDM symbols  $u(t, \mathbf{b})$  given in (1) which is defined as

$$\xi_N(\mathbf{b}) = \max_{t \in [0, T)} |u(t, \mathbf{b})|^2.$$

Clearly, for any finite oversampling factor  $L$ ,

$$\theta_N(\mathbf{b}) \leq \xi_N(\mathbf{b}).$$

Therefore, It directly follows from (13) that

$$\frac{\theta_N(\mathbf{b} \odot \mathbf{x}^*) - a_N}{b_N} \leq \mathbb{E}_{\mathbf{X}} \left[ \frac{\xi_N(\mathbf{b} \odot \mathbf{X}) - a_N}{b_N} \right]$$

for any  $N$ . Therefore [27],

$$\lim_{N \rightarrow \infty} \frac{\theta_N(\mathbf{b} \odot \mathbf{x}^*) - a_N}{b_N} \leq \lim_{N \rightarrow \infty} \mathbb{E}_{\mathbf{X}} \left[ \frac{\xi_N(\mathbf{b} \odot \mathbf{X}) - a_N}{b_N} \right]. \quad (29)$$

In order to obtain the right hand side limit, recall that the covariance functions of  $u(t, \mathbf{b} \odot \mathbf{X})$ , as emphasized in Remark 1, was shown to be identical to that of  $u(t, \mathbf{B})$  as  $N \rightarrow \infty$ . In addition, Extreme Value Theory [28] has been employed in [29] to obtain the asymptotic distribution of  $\xi_N(\mathbf{B})$  as

$$\lim_{N \rightarrow \infty} \mathbb{P} \left( \frac{\xi_N(\mathbf{B}) - b_N}{a_N} \leq w \right) = e^{-e^{-w}}.$$

That is, the appropriately shifted and scaled variable  $\xi_N(\mathbf{B})$  has Gumbel distribution in the limit. Consequently, the results of [29] hold for the asymptotic distribution of  $u(t, \mathbf{b} \odot \mathbf{X})$  as well and

$$\lim_{N \rightarrow \infty} \mathbb{P} \left( \frac{\xi_N(\mathbf{b} \odot \mathbf{X}) - b_N}{a_N} \leq w \right) = e^{-e^{-w}}.$$

Finally, the expected value of a random variable with the Gumbel distribution is

$$\lim_{N \rightarrow \infty} \mathbb{E}_{\mathbf{X}} \left[ \frac{\xi_N(\mathbf{b} \odot \mathbf{X}) - a_N}{b_N} \right] = \gamma,$$

which is the right hand side of (29). This completes the proof.  $\square$

The asymptotic result in Theorem 3 shows an upperbound for  $\theta_N(\mathbf{B} \odot \mathbf{x}^*)$  when shifted by  $a_N$  which grows with  $N$ . This implies an approximate inequality for finite but large  $N$ , as stated below.

**Remark 3.** *For large enough  $N$ , Theorem 3 implies the upperbound*

$$\theta_N(\mathbf{b} \odot \mathbf{x}^*) \leq \log N + \frac{1}{2} \log \log N + K \quad (30)$$

for any  $\mathbf{b} \in \mathcal{M}^N$ , where  $K = \frac{1}{2} \log \frac{\pi}{3} + \gamma \simeq 0.59$ .

Since the upperbound of Theorem 3 holds for every  $\mathbf{b} \in \mathcal{M}^N$ , it is equivalently an upperbound on the worst-case reduced PAPR value, i.e.  $\theta_N^{\max} = \max_{\mathbf{b} \in \mathcal{M}^N} \theta_N(\mathbf{b} \odot \mathbf{x}^*)$ . Except for relatively small  $N$ , it is not feasible to observe  $\theta_N^{\max}$  in the actual performance investigation by computer simulations or in practice. Instead, it is common to measure the *effective reduced PAPR*  $\theta_N^{\text{eff}}$  which is defined according to

$$\mathbb{P}\{\theta_N(\mathbf{B} \odot \mathbf{x}^*) > \theta_N^{\text{eff}}\} = 0.001. \quad (31)$$

Although it can intuitively be expected that  $\theta_N^{\text{eff}}$  is much smaller than  $\theta_N^{\max}$ , a formal relation is not available.

### B. Cubic Metric

The following theorem was previously presented by the authors in [26], which obtains a constant upperbound on the reduced SRCM value.

**Theorem 4.** *The reduced SRCM value  $\eta_N(\mathbf{b} \odot \mathbf{x}^*)$  obtained by the CE Method is bounded in the limit as*

$$\lim_{N \rightarrow \infty} \eta_N(\mathbf{b} \odot \mathbf{x}^*) \leq 6 \quad (32)$$

for any  $\mathbf{b} \in \mathcal{M}^N$ .

*Proof.* As stated in (13), the CE Method guarantees that

$$\eta_N(\mathbf{b} \odot \mathbf{x}^*) \leq \mathbb{E}_{\mathbf{X}}[\eta_N(\mathbf{b} \odot \mathbf{X})]. \quad (33)$$

From the definition of SRCM in (6), we have  $\mathbb{E}[\eta_N(\mathbf{b})] = \frac{1}{LN} \sum_{n=0}^{LN-1} \mathbb{E}[|s(n, \mathbf{b})|^6]$ . In addition, it can be concluded from Remark 1 that the distribution of the discrete-time signal  $s(n, \mathbf{b} \odot \mathbf{X})$  in the limit is the same as that of  $s(n, \mathbf{B})$ . Therefore,

$$\lim_{N \rightarrow \infty} \mathbb{E}_{\mathbf{X}}[\eta_N(\mathbf{b} \odot \mathbf{X})] = \lim_{N \rightarrow \infty} \mathbb{E}[\eta_N(\mathbf{B})]. \quad (34)$$

The distribution of  $\eta_N(\mathbf{B})$  is studied in [19], where it is shown that

$$\lim_{N \rightarrow \infty} \mathbb{E}[\eta_N(\mathbf{B})] = 6.$$

Considering (33), (34) and that an inequality between two sequences is preserved in their limits [27], we have

$$\lim_{N \rightarrow \infty} \eta_N(\mathbf{b} \odot \mathbf{x}^*) \leq \lim_{N \rightarrow \infty} \mathbb{E}[\eta_N(\mathbf{B})],$$

which completes the proof.  $\square$

Recall that the reduction of RCM is the actual objective sought in reduction of SRCM and that CM is related to RCM by some constants. Clearly, Theorem 4 shows an upperbound on the largest or worst-case reduced SRCM. Being equal to the average of the reduced SRCM values, RCM can be expected to be much smaller than the upperbound unless the distribution of  $\eta_N(\mathbf{B} \odot \mathbf{x}^*)$  is highly concentrated. Similar to the relation of the effective reduced PAPR and the upperbound, further characterization of RCM reduction is not available.

## VI. SIMULATION RESULTS AND DISCUSSION

In this section, the performance of the CE method in reducing PAPR and CM is examined via simulation results. The performance here refers to the reduction in the metrics of interest achieved by the suboptimal solution to the Sign Selection problem, including the indirect PAPR reduction gained by applying the proposed method to the SE metric.

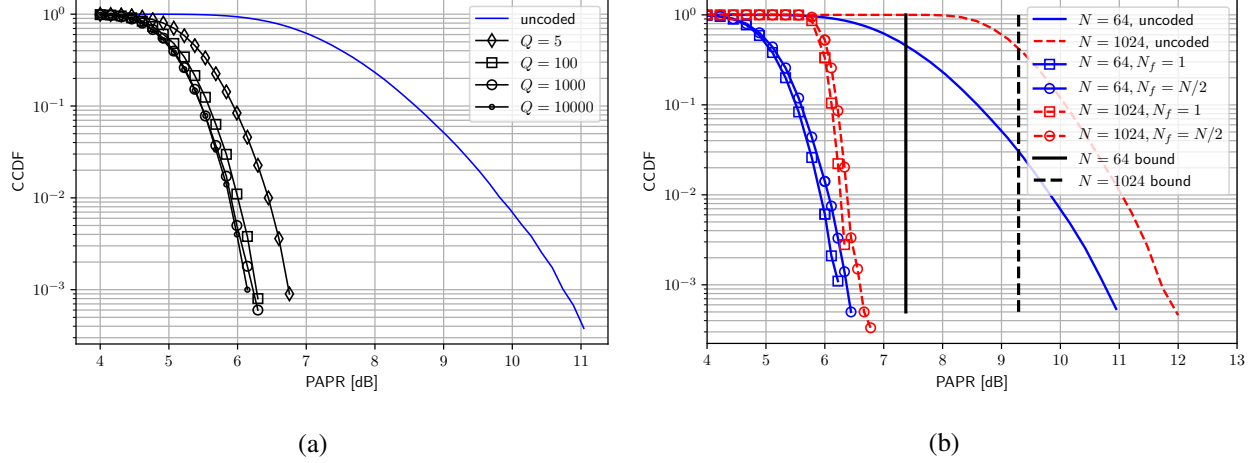


Fig. 2: a) Reduction performance of the CE method for PAPR for various number of shots  $Q$ , as defined in (18), to show the reliability of estimation for  $N = 64$  and 16-QAM. b) Reduction performance of the CE method for PAPR with 16-QAM and  $Q = 100$ , including analytical upperbound of (30) on the worst-case reduced PAPR value.

#### A. PAPR reduction

The Complementary Cumulative Distribution Function (CCDF) of  $\theta_N(\mathbf{B})$ , i.e.  $\mathbb{P}(\theta_N(\mathbf{B}) > y)$ , with  $\mathbf{B} \in \mathcal{M}^N$  is commonly used to represent the *uncoded PAPR*, i.e. the PAPR of an unprocessed signal. Accordingly, the reduction performance is reported by the CCDF of  $\theta_N(\mathbf{B} \odot \mathbf{x}^*)$  for  $\mathbf{B} \in \mathcal{M}^N$ . To report the performance in the text, the *effective PAPR* is used which is the PAPR value where CCDF equals 0.001.

a) *Choice of  $Q$* : To investigate the reliability of the estimations required in the sign selection rule for PAPR given in (18), the reduction performance gained by several values of  $Q$  for  $N = 64$  is depicted in Fig. 2a. It was observed that the difference for  $Q \geq 100$  was insignificant. Consequently,  $Q = 100$  has been used in the rest of the simulations. As a side note, a very low value of  $Q = 5$  was included in the figure to show the unexpectedly acceptable reduction that it provides.

b) *Dependence on  $N$* : The PAPR reduction performance of the algorithm is shown in Fig. 2b for  $N = 64$  and 1024 subcarriers, including its pruned version which will be shortly introduced. The simulation results are depicted only for 16-QAM as similar results were observed for other constellations. A significant reduction gain of roughly 5.5 dB, equivalently an effective

PAPR of 6.5 dB, was observed for  $N = 1024$ . A noticeable characteristic of the method, evident from the simulations, is that the change in the reduced effective PAPR is relatively small by increasing  $N$  from 64 to 1024.

The analytic upper bound on the worst-case reduced PAPR, as shown in Theorem 3 and given in (30), is included in Fig. 2b. The proof of Theorem 3 relies on the extremal value theory to analyze the expected value of the uncoded PAPR, i.e.  $\mathbb{E}[\theta_N(\mathbf{B})]$  as  $N \rightarrow \infty$ . The usefulness of this asymptotic result for  $\mathbb{E}[\theta_N(\mathbf{B})]$  with finite  $N$  can be asserted as (30) is almost equal to a diligently calculated empirical average of  $\theta_N(\mathbf{B})$  for  $N$  as small as 64. Refer to the discussion in Section V regarding the relationship between the upperbound and the effective reduced PAPR.

*c) Pruned Sign Selection and Rate loss:* It has been observed through simulations that the impact of a sign decision increases for the sign variables with higher indices. That is, the reduction steps in the trajectory of the conditional expectations, as the algorithm performs sign decisions for  $x_0$  to  $x_{N-1}$ , become statistically larger. This motivates pruning the sign bits whose contribution is insignificant. Formally, in the *pruned Sign Selection*,  $x_{0:N_f-1}^*$  are set as the signs of the first  $N_f$  symbols which fully carry data and the sign bits of  $N - N_f$  last symbols are determined by (11).

The pruned algorithm with  $N_f = \frac{N}{2}$ , as shown in Fig. 2b, causes negligible degradation in the reduction performance while reducing the rate loss of the Sign Selection approach. Evident from (10), the rate loss is inversely related to the constellation size  $|\mathcal{M}|$ . Accordingly, the rate loss is  $\frac{1}{12}$ ,  $\frac{1}{8}$  and  $\frac{1}{4}$  for  $N_f = \frac{N}{2}$  and 64-QAM, 16-QAM and QPSK respectively. Obviously, a lower rate loss implies a smaller number of sign selections, hence a lower computational complexity.

*d) Indirect PAPR reduction by SE Metric:* As discussed in Section IV-C, the first  $N - N_e$  signs decisions for reduction of the SE metric can be done by the rule in (26) and the last  $N_e$  are done by (15), where the latter is based on the estimation of the conditional expectations. The choice of  $N_e$  depends on  $Q$ , i.e. the number of the realizations of the random sign vector used in the estimation. For a given  $Q$ , a number of the early decisions are done more accurately using closed-form expressions of (26). When the number of remaining signs is low enough, the accuracy of the estimation overcomes. This intuition was evaluated for SE by examining the reduction performance for  $N = 64$  and  $Q = 10, 100, 10000$  for  $N_e = 0, 5, 10$  and 20. The relatively small  $N$  was chosen on purpose to have a smaller number of total random variables. It was observed that the effective PAPR reduces from roughly 8.5 dB for  $N_e = 0$  to 6.8 dB for  $N_e = 10$  which was better than both 5 and 20 with effective PAPR of roughly 7.1 and 7 dB.

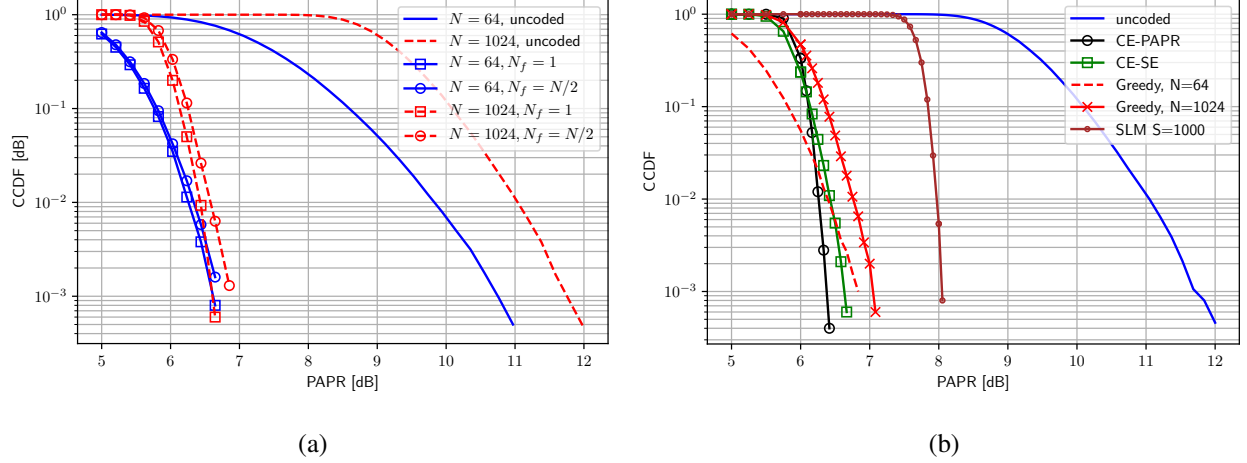


Fig. 3: a) Indirect PAPR reduction by pruned application of the CE method to SE for 16-QAM with  $\kappa = 10$ ,  $N_e = 10$ ,  $Q = 100$ . b) Reduction performance of the CE method applied to PAPR (CE-PAPR) and SE (CE-SE) compared to Greedy Algorithm [15] and Selected Mapping (SLM).  $N = 1024$  unless stated otherwise.

In addition, going from  $Q = 10$  to  $Q = 10000$  showed insignificant effect. As a conclusion,  $N_e = 10$  and  $Q = 100$  were selected.

The indirect PAPR reduction achieved by reduction of the SE metric is shown in Fig. 3a for  $N = 64$  and 1024. Although increasing the parameter  $\kappa$  improves the SE metric in theory, numerical computations limit its value. Thus,  $\kappa = 10$  was chosen. It can be seen that the indirect PAPR reduction is as strong as the direct one showing a relatively small degradation. The pruning idea works as well, showing that only a slight loss in gain occurs when rate loss is halved.

*e) Comparison:* It is a rather common characteristic of the PAPR reduction methods in the literature that the reduced PAPR grows larger as  $N$  increases. The CE method differs in this regards such that, as mentioned before, the reduced effective PAPR increases only slightly by  $N$ . Among the Sign Selection methods, a competitive proposal referred to as the Greedy Algorithm [15] was chosen for comparison. The well-known Selected Mapping (SLM) [5] with sign flips as phase rotations was also included, which can as well be seen as a Sign Selection method. The results are gathered in Fig. 3b, where it can be seen that the Greedy Algorithm performs better for  $N = 64$  but falls behind for  $N = 1024$ . The performance of SLM depends on the number of independent mappings of the signal denoted by  $S$ . For the considerably large  $S = 1000$ , the reduction gained by SLM is far lower. As a matter of fact, the performance of

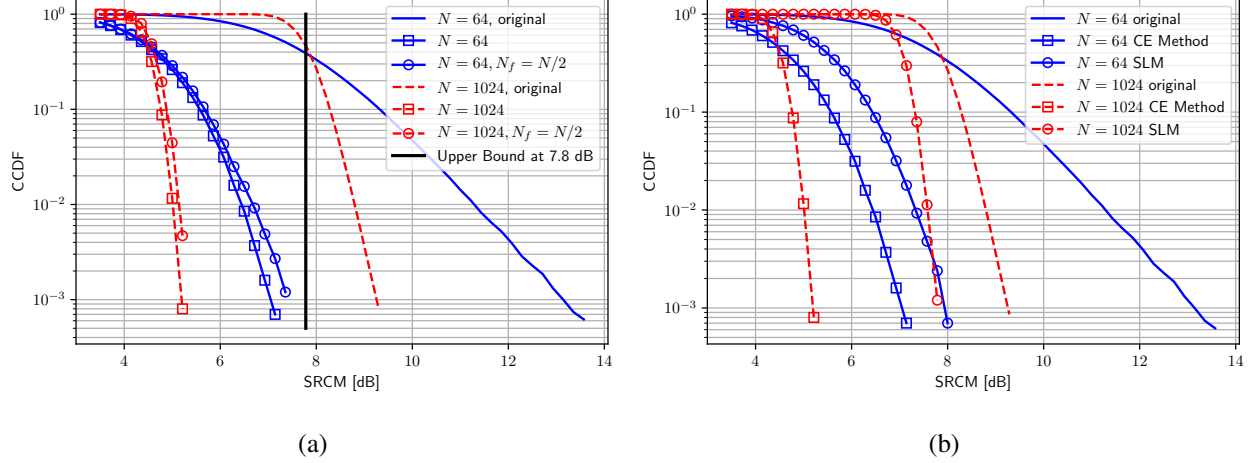


Fig. 4: a) Reduction performance by pruned CE method applied to SRCM for 16-QAM, including the analytical upperbound on the worst-case reduced metric value. b) Comparison of the SRCM reduction performance of CE Method and SLM with  $S = 100$ .

SLM can be shown to improve only slightly by increasing  $S$  indicating its inherent limitation. The gap becomes larger for higher  $N$ .

### B. Cubic Metric

Reduction performance for SRCM is shown in Fig. 4a for  $N = 64$  and  $1024$  to cover a wide range of subcarrier numbers. As shown in the figure, the performance of the pruned algorithm with  $N_f = \frac{N}{2}$ , i.e. using the second half of sign bits, is only slightly degraded compared to the  $N_f = 0$  case. This reconfirms the result seen before in PAPR reduction that the proposed algorithm provides almost the same reduction by half the full rate loss, i.e.  $\frac{1}{2} \log_{|M|} 2$ .

The analytical upperbound of Theorem 4 is as well included in Fig. 4a. The upperbound on the worst-case reduced SRCM is the expected value of the uncoded SRCM, i.e.  $\mathbb{E}[\eta_N(\mathbf{B})]$  as  $N \rightarrow \infty$ . The reliability of this asymptotic result was observed as it matches very closely with the empirical average of  $\eta_N(\mathbf{B})$  particularly when  $N$  is larger than 64. Similar to the PPAR reduction, the simulation results show a growing reduction gain as  $N$  increases. The difference in the SRCM case is that the upperbound is independent of  $N$ , therefore the reduced effective SRCM decreases, which implies the growing reduction gain.

Recall that the main metric of interest is CM which is calculated from RCM by knowing hardware-related constants. Therefore, we suffice to reporting RCM, which is the expected value

TABLE I: RCM Reduction Performance.

$N$	original RCM	original CM	reduced RCM	reduced CM
64	7.7 dB	-	4.5 dB	-
512	7.8 dB	4.8 dB	4.5 dB	2.87 dB
1024	7.8 dB	-	4.5 dB	-

of SRCM as in (7). RCM is reduced roughly from 7.7 dB to 4.5 dB for both  $N = 64$  and 1024. That is, a surprising result of nearly 3.2 dB reduction practically regardless of  $N$ . For  $N = 512$ , which is the case studied in [21] with available  $K_{\text{slp}}$  and  $K_{\text{bw}}$ , the CM is reduced to 2.87 dB. The available values are presented in Table I.

Due to the scarcity of research on CM reduction, we sufficed to the well-known SLM method [5] for comparison. The result is shown in Fig. 4b for the relatively large  $S = 100$ . For both cases of  $N = 64$  and 1024, performance of the proposed algorithm is significantly better than SLM.

## VII. CONCLUSION

The Method of Conditional Expectations was proposed to find a suboptimal solution to the Sign Selection problem. This investigation led to three particular observations. Firstly, using the conditional expectations as the core element of the sign selection rules provides room for reducing complexity of the algorithm. In particular, proposal of the SE metric as a surrogate function to PAPR led to closed-form expressions for sign selection rule and negligible loss in performance. A similar observation was done for CM which inherently has a tractable definition. This motivates creativity in developing surrogate functions to replace the metrics with physical significance, i.e. PAPR and CM. Secondly, the structure of the CE Method permits derivation of a meaningful upperbound on the largest reduced metric value, such that it actually guarantees a minimum reduction on the effective metric value. Thirdly, the actual performance observed by simulations show a remarkable reduction which is persistent as  $N$  increases. In addition, the reduction gain deteriorates only slightly when reducing the number of used sign bits to half, which implies a significantly lower rate loss.



## APPENDIX A

## PROOF OF THEOREM 1

Recall the random vectors  $\mathbf{X}^l \in \{-1, 1\}^{N-j-1}, l = 1, \dots, Q$  with independent elements as used in the definition of  $\hat{g}_j^\pm(\mathbf{b}, \mathbf{X}^{1:Q})$  in (18). Suppose that the real-valued function  $\hat{g}_j^+$  satisfies

$$|\hat{g}_j^+(\mathbf{b}, \mathbf{v}^{1:Q}) - \hat{g}_j^+(\mathbf{b}, \mathbf{z}^{1:Q})| \leq d_{m,k} \quad (35)$$

when vectors  $\mathbf{v}^l, \mathbf{z}^l \in \{-1, 1\}^{N-j-1}, l = 1, 2, \dots, Q$  disagree only at  $v_k^m = -z_k^m$ . Then for any  $\epsilon \geq 0$ , McDiarmid's *independent bounded differences* inequality [24, p. 206] holds as

$$\mathbb{P}(|\hat{g}_j^+(\mathbf{b}, \mathbf{X}^{1:Q}) - g_j^+(\mathbf{b})| \geq \epsilon) \leq 2e^{-2\epsilon^2(\sum_{m,k} d_{m,k}^2)^{-1}},$$

where  $g_j^+(\mathbf{b}) = \mathbb{E}[\hat{g}_j^+(\mathbf{b}, \mathbf{X}^{1:Q})]$ .

The bounded differences of (35) on  $\hat{g}_j^+$  can be shown as follows.

$$\begin{aligned} |\hat{g}_j^+(\mathbf{b}, \mathbf{v}^{1:Q}) - \hat{g}_j^+(\mathbf{b}, \mathbf{z}^{1:Q})| &= \left| \frac{1}{Q} \sum_{l=1}^Q [\theta_N(\mathbf{b} \odot \psi_j^+(\mathbf{v}^l)) - \theta_N(\mathbf{b} \odot \psi_j^+(\mathbf{z}^l))] \right| \\ &\leq \frac{1}{Q} \sum_{l=1}^Q \left| \max_n |s(n, \mathbf{b} \odot \psi_j^+(\mathbf{v}^l))| - \max_n |s(n, \mathbf{b} \odot \psi_j^+(\mathbf{z}^l))| \right| \\ &\leq \frac{1}{Q} \sum_{l=1}^Q \max_n |s(n, \mathbf{b} \odot \psi_j^+(\mathbf{v}^l)) - s(n, \mathbf{b} \odot \psi_j^+(\mathbf{z}^l))| \\ &= \frac{1}{Q} \frac{1}{\sqrt{N}\sigma_b} 2|b_m| \leq \frac{1}{Q} \frac{1}{\sqrt{N}} d \end{aligned} \quad (36)$$

where

$$\left| \max_n |p(n)| - \max_n |q(n)| \right| \leq \max_n |p(n) - q(n)|$$

is used and  $d = 2\sigma_b^{-1} \max_{x \in \mathcal{M}} |x|$ . Therefore,  $\sum_{m,k} d_{m,k}^2 = Q \frac{N-j-1}{N} d$ , which completes the proof for  $\hat{g}_j^+$ . Similar steps can be taken to proof the result for  $\hat{g}_j^-$ .

## APPENDIX B

## PROOF OF LEMMA 1

A.  $R_{ri}(\mathbf{B}, \tau)$  a Gaussian random variable

We begin the proof by analyzing  $R_{ri}^j(\tau, \mathbf{B})$  at iteration  $j$  of the CE Method and for the random vector of data symbols  $\mathbf{B} \in \mathcal{M}^N$  which was defined in Lemma 1 and is rewritten here as

$$R_{ri}^j(\tau, \mathbf{B}) = \lim_{N \rightarrow \infty} h_N^{ri}(\mathbf{B}, t_1, t_2), \quad (37)$$

where  $\tau = t_2 - t_1$  and

$$h_N^{ri}(\mathbf{B}, t_1, t_2) = \mathbb{E}_{\mathbf{Y}_j^\pm} [\hat{u}_r(t_1, \mathbf{B} \odot \mathbf{Y}_j^\pm) \hat{u}_i(t_2, \mathbf{B} \odot \mathbf{Y}_j^\pm)]. \quad (38)$$

Based on the definition of the signal  $u$  in (1),

$$\begin{aligned} h_N^{ri}(\mathbf{B}, t_1, t_2) &= \frac{1}{N\sigma_b^2} \mathbb{E}_{X_{j+1:N-1}} \left[ \sum_{k_1=j+1}^{N-1} \sum_{k_2=j+1}^{N-1} X_{k_1} \operatorname{Re}\{B_{k_1} e^{i\omega_{k_1} t_1}\} X_{k_2} \operatorname{Im}\{B_{k_2} e^{i\omega_{k_2} t_2}\} \right] \\ &= \frac{1}{N\sigma_b^2} \sum_{k=j+1}^{N-1} \operatorname{Re}\{B_k e^{i\omega_k t_1}\} \operatorname{Im}\{B_k e^{i\omega_k t_2}\}, \end{aligned} \quad (39)$$

where  $\omega_k = \frac{2\pi}{N} F_s k$  and the independence of the random sign variables  $X_{j+1:N-1}$  in  $\mathbf{Y}_j^\pm$  is used.

At this juncture, the relation of  $j$  and  $N$  must be reviewed. Consider two cases: If  $j$  remains constant while  $N$  grows, it can be easily seen from the following derivations that the desired quantities are identical in the limit, i.e. as  $N \rightarrow \infty$ , to the case where no sign decision is made by the CE Method. The second case is when  $j$  grows with  $N$ , which needs attention and is the assumption in Lemma 1. Specifically, as introduced in Lemma 1,  $j = \rho N$  where  $0 \leq \rho \leq 1$  is a constant rational number.

Since the summands in (39) are independent, it is straightforward to apply the Central Limit Theorem to show that  $h_N^{ri}(\mathbf{B}, t_1, t_2)$  converges in distribution to a Gaussian random variable as  $N \rightarrow \infty$ . That is,

$$R_{ri}^j(\tau, \mathbf{B}) \sim \mathcal{N}(\mu_{ri}(\tau), \sigma_{ri}^2), \quad (40)$$

where

$$\mu_{ri}(\tau) = \lim_{N \rightarrow \infty} \mathbb{E}[h_N^{ri}(\mathbf{B}, t_1, t_2)] \quad (41)$$

and

$$\sigma_{ri}^2 = \lim_{N \rightarrow \infty} \mathbb{E}[(h_N^{ri}(\mathbf{B}, t_1, t_2))^2] - (\mu_{ri}(\tau))^2. \quad (42)$$

Next we derive  $\mu_{ri}(\tau)$  and show that  $\sigma_{ri}^2 = 0$ , which implies that  $R_{ri}^j(\tau, \mathbf{B})$  is equal to  $\mu_{ri}(\tau)$  with probability one.

### B. Convergence of $\mu_{ri}(\tau)$

Given the independence of the data symbols, we have

$$\mathbb{E}[h_N^{ri}(\mathbf{B}, t_1, t_2)] = \frac{1}{2N} \sum_{k=j+1}^{N-1} a_k,$$

where

$$a_k = \cos(\omega_k t_1) \sin(\omega_k t_2) + \sin(\omega_k t_1) \cos(\omega_k t_2).$$

Consequently,

$$\begin{aligned} \mathbb{E}[h_N^{ri}(\mathbf{B}, t_1, t_2)] &= \frac{1}{2N} \sum_{k=j+1}^{N-1} \sin(\omega_k \tau) \\ &= \frac{1}{2N} \sum_{k=0}^{N-1} \sin(\omega_k \tau) - \frac{1}{2} \frac{j}{N} \frac{1}{j} \sum_{k=0}^j \sin(\omega_k \tau). \end{aligned} \quad (43)$$

where  $\tau = t_2 - t_1$ . Consider the series

$$\alpha_M = \frac{1}{2M} \sum_{k=0}^{M-1} \sin\left(\frac{2\pi}{M} k F_s \tau\right) \quad (44)$$

which can be shown to converge as

$$\lim_{M \rightarrow \infty} \alpha_M = \frac{1}{4\pi F_s \tau} (1 - \cos(2\pi F_s \tau)), \quad \tau \neq 0.$$

Recall that  $j = \rho N$ , where  $\rho = \frac{m}{p}$  is an irreducible fraction, dictates that  $N$  grows as  $N = m, 2m, \dots$  with  $m \in \mathbb{N}$ . Consequently, the first series in (43), i.e.

$$\beta_N = \frac{1}{2N} \sum_{k=0}^{N-1} \sin\left(\frac{2\pi}{N} k F_s \tau\right), \quad N = m, 2m, \dots$$

is a subsequence of  $\{\alpha_M\}$ , which readily shows that [27]

$$\lim_{N \rightarrow \infty} \beta_N = \lim_{M \rightarrow \infty} \alpha_M.$$

Rewriting  $\frac{2\pi}{N}$  as  $\frac{2\pi}{j} \frac{j}{N} = \frac{2\pi}{j} \rho$ , the second series in (43) can be written as

$$\zeta_j = \frac{1}{j} \sum_{k=0}^j \sin\left(\frac{2\pi}{j} \rho F_s k \tau\right), \quad j = p, 2p, \dots$$

Then  $\zeta_j$  is a subsequence of a sequence similar to  $\{\alpha_M\}$  and consequently

$$\lim_{j \rightarrow \infty} \zeta_j = \frac{1}{4\pi F_s \rho \tau} (1 - \cos(2\pi F_s \rho \tau)), \quad \tau \neq 0$$

Therefore, (43) converges. Substituting the limit in (41), we have

$$\mu_{ri}(\tau) = \begin{cases} \frac{1}{4\pi F_s \tau} \left( \frac{1}{\rho} \cos(2\pi F_s \rho \tau) - \cos(2\pi F_s \tau) \right) & \tau \neq 0 \\ 0 & \tau = 0 \end{cases} \quad (45)$$

where the case of  $\tau = 0$  is trivial.

### C. Convergence of $\sigma_{ri}^2$ to zero

Consider that

$$(h_N^{ri}(\mathbf{B}, t_1, t_2))^2 = \frac{1}{N^2 \sigma_b^4} \left( \sum_{k=j}^{N-1} [B_k^r \cos(\omega_k t_1) - B_k^i \sin(\omega_k t_1)] [B_k^r \sin(\omega_k t_2) - B_k^i \cos(\omega_k t_2)] \right)^2$$

where  $B_k^r = \text{Re}[B_k]$  and  $B_k^i = \text{Im}[B_k]$ . By some manipulations which are omitted for the sake brevity, we have

$$\begin{aligned} \mathbb{E} \left[ (h_N^{ri}(\mathbf{B}, t_1, t_2))^2 \right] &= \frac{1}{N^2 \sigma_b^4} \left( \frac{\sigma_b^4}{4} \left( \sum_{k=j}^{N-1} a_k \right)^2 - \frac{\sigma_b^4}{4} \sum_{k=j}^{N-1} a_k^2 \right. \\ &\quad + \gamma \sum_{k=j}^{N-1} [(\cos(\omega_k t_1) \sin(\omega_k t_2))^2 + (\cos(\omega_k t_2) \sin(\omega_k t_1))^2] \\ &\quad \left. - \frac{\sigma_b^4}{2} \sum_{k=j}^{N-1} \cos(\omega_k t_1) \cos(\omega_k t_2) \sin(\omega_k t_1) \sin(\omega_k t_2) \right), \end{aligned} \quad (46)$$

and  $\gamma = \mathbb{E}[(B_k^r)^4]$ . Notice that all summands in the four summations of (46) are bounded. For instance,  $\frac{1}{N^2} \sum_{k=j}^{N-1} a_k^2 \leq \frac{1}{N} A$  with  $a_k^2 \leq A$  for some  $A \geq 0$ . Consequently, the non-negative series  $\frac{1}{N^2} \sum_{k=j}^{N-1} a_k^2$  converges to zero. By the same argument, the third and fourth summations in (46) vanish in the limit too. That is,

$$\lim_{N \rightarrow \infty} \mathbb{E} \left[ (h_N^{ri}(\mathbf{B}, t_1, t_2))^2 \right] = \lim_{N \rightarrow \infty} \left( \frac{1}{2N} \sum_{k=j}^{N-1} a_k \right)^2. \quad (47)$$

It was already shown in derivation of  $\mu_{ri}(\tau)$  that  $\frac{1}{N} \sum_{k=j}^{N-1} a_k$  converges. Therefore, [27]

$$\lim_{N \rightarrow \infty} \left( \frac{1}{2N} \sum_{k=j}^{N-1} a_k \right)^2 = \left( \lim_{N \rightarrow \infty} \frac{1}{2N} \sum_{k=j}^{N-1} a_k \right)^2 = (\mu_{ri}(\tau))^2.$$

Finally,

$$\sigma_{ri}^2 = \lim_{N \rightarrow \infty} \left( \frac{1}{2N} \sum_{k=j}^{N-1} a_k \right)^2 - (\mu_{ri}(\tau))^2 = 0. \quad (48)$$

Consequently, we have shown that  $R_{ri}(\mathbf{B}, \tau)$  is an *almost surely constant* random variable and  $R_{ri}(\mathbf{B}, \tau) = \mu_{ri}(\tau)$  with probability one. This completes the proof for  $R_{ri}(\mathbf{B}, \tau)$ .

#### D. $R_{rr}(\mathbf{B}, \tau)$ and $R_{ii}(\mathbf{B}, \tau)$

Similarly, for  $R_{rr}(\mathbf{B}, \tau)$  we have

$$h_N^{rr}(\mathbf{B}, t_1, t_2) = \mathbb{E} [\hat{u}_r(t_1, \mathbf{B} \odot \mathbf{Y}_j^\pm) \hat{u}_r(t_2, \mathbf{B} \odot \mathbf{Y}_j^\pm)] = \frac{1}{N\sigma_b^2} \sum_{k=j}^{N-1} \text{Re}\{b_k e^{i\omega_k t_1}\} \text{Re}\{b_k e^{i\omega_k t_2}\}$$

with

$$\begin{aligned} \mu_{rr}(\tau) &= \lim_{N \rightarrow \infty} \mathbb{E} [h_N^{rr}(\mathbf{B}, t_1, t_2)] \\ &= \frac{1}{2} \lim_{N \rightarrow \infty} \frac{1}{N} \sum_{k=j}^{N-1} \cos(\omega_k \tau) \\ &= \frac{1}{2} (\text{sinc}(2F_s \tau) - \rho \text{sinc}(2F_s \tau \rho)). \end{aligned} \quad (49)$$

Following the steps taken to derive (48), we have

$$\sigma_{rr}^2 = \lim_{N \rightarrow \infty} \mathbb{E} [(h_N^{rr}(\mathbf{B}, t_1, t_2))^2] - (\mu_{rr}(\tau))^2 = 0,$$

which implies that  $R_{rr}(\mathbf{B}, \tau) = \mu_{rr}(\tau)$  with probability one and completes the proof. Finally, the derivations for  $R_{ii}(\mathbf{B}, \tau)$  are identical to that of  $R_{rr}(\mathbf{B}, \tau)$ .

#### REFERENCES

- [1] M.-o. Pun, M. Morelli, and C. C. J. Kuo, *Multi-Carrier Techniques For Broadband Wireless Communications: A Signal Processing Perspectives*. London, UK, UK: Imperial College Press, 2007.
- [2] H. Ekstrom, A. Furuskar, J. Karlsson, M. Meyer, S. Parkvall, J. Torsner, and M. Wahlqvist, "Technical solutions for the 3G long-term evolution," *IEEE Communications Magazine*, vol. 44, no. 3, pp. 38–45, March 2006.
- [3] Motorola, "Comparison of PAR and Cubic Metric for Power De-rating," 3GPP TSG-RAN WG1 LTE, Tech. Rep., May 2004, tdoc R1-040642.
- [4] J. Armstrong, "Peak-to-average power reduction for OFDM by repeated clipping and frequency domain filtering," *Electronics Letters*, vol. 38, no. 5, pp. 246–247, Feb 2002.
- [5] R. Bauml, R. F. H. Fischer, and J. Huber, "Reducing the peak-to-average power ratio of multicarrier modulation by selected mapping," *Electronics Letters*, vol. 32, no. 22, pp. 2056–2057, Oct 1996.
- [6] J. Tellado, *Multicarrier Modulation with Low PAR: Applications to DSL and Wireless*. Kluwer Academic Publishers, 2000.
- [7] S. H. Han and J. H. Lee, "An overview of peak-to-average power ratio reduction techniques for multicarrier transmission," *Wireless Communications, IEEE*, vol. 12, no. 2, pp. 56–65, April 2005.
- [8] G. Wunder, R. F. H. Fischer, H. Boche, S. Litsyn, and J.-S. No, "The PAPR problem in OFDM transmission: New directions for a long-lasting problem," *The IEEE signal processing magazine*, vol. abs/1212.2865, 2013.
- [9] M. Deumal, A. Behravan, and J. L. Pijoan, "On Cubic Metric Reduction in OFDM Systems by Tone Reservation," *IEEE Transactions on Communications*, vol. 59, no. 6, pp. 1612–1620, June 2011.

- [10] X. Zhu, H. Hu, and Y. Tang, "Descendent clipping and filtering for cubic metric reduction in OFDM systems," *Electronics Letters*, vol. 49, no. 9, pp. 599–600, April 2013.
- [11] A. Skrzypczak, P. Siohan, and J. Javardin, "Power Spectral Density and Cubic Metric for the OFDM/OQAM Modulation," in *2006 IEEE International Symposium on Signal Processing and Information Technology*, Aug 2006, pp. 846–850.
- [12] M. Sharif and B. Hassibi, "Existence of codes with constant PMEPR and related design," *Signal Processing, IEEE Transactions on*, vol. 52, no. 10, pp. 2836–2846, Oct 2004.
- [13] S. Afrasiabi Gorgani and G. Wunder, "Derandomized multi-block sign selection for PMEPR reduction of FBMC waveform," in *Vehicular Technology Conference (VTC Spring), 2015 IEEE 81th*, May 2015.
- [14] L. Wang and C. Tellambura, "Clipping-Noise Guided Sign-Selection for PAR Reduction in OFDM Systems," *IEEE Transactions on Signal Processing*, vol. 56, no. 11, pp. 5644–5653, Nov 2008.
- [15] M. Sharif, V. Tarokh, and B. Hassibi, "Peak power reduction of OFDM signals with sign adjustment," *Communications, IEEE Transactions on*, vol. 57, no. 7, pp. 2160–2166, July 2009.
- [16] L. Wang and C. Tellambura, "Cross-Entropy-Based Sign-Selection Algorithms for Peak-to-Average Power Ratio Reduction of OFDM Systems," *IEEE Transactions on Signal Processing*, vol. 56, no. 10, pp. 4990–4994, Oct 2008.
- [17] M. Mitzenmacher and E. Upfal, *Probability and computing : randomized algorithms and probabilistic analysis*. New York: Cambridge University Press. [Online]. Available: <http://opac.inria.fr/record=b1117540>
- [18] G. Wunder and H. Boche, "Peak value estimation of bandlimited signals from their samples, noise enhancement, and a local characterization in the neighborhood of an extremum," *Signal Processing, IEEE Transactions on*, vol. 51, no. 3, pp. 771–780, March 2003.
- [19] K. H. Kim, J. S. No, and D. J. Shin, "On the Properties of Cubic Metric for OFDM Signals," *IEEE Signal Processing Letters*, vol. 23, no. 1, pp. 80–83, Jan 2016.
- [20] S. Boyd and L. Vandenberghe, *Convex Optimization*. New York, NY, USA: Cambridge University Press, 2004.
- [21] Motorola, "Cubic Metric in 3GPP LTE," 3GPP TSG-RAN WG1 LTE, Tech. Rep., Jan 2006, tdoc R1-060023.
- [22] S. Benedetto and E. Biglieri, *Principles of Digital Transmission: With Wireless Applications*. Norwell, MA, USA: Kluwer Academic Publishers, 1999.
- [23] S. Afrasiabi-Gorgani and G. Wunder, "A Versatile PAPR Reduction Algorithm for 5G Waveforms with Guaranteed Performance," in *WSA 2016; 20th International ITG Workshop on Smart Antennas; Proceedings of*, March 2016.
- [24] M. Habib, C. McDiarmid, J. Ramirez-Alfonsin, and B. Reed, *Probabilistic Methods for Algorithmic Discrete Mathematics*. Springer-Verlag Berlin Heidelberg, 1998.
- [25] P. Billingsley, *Convergence of probability measures*, 2nd ed. John Wiley & Sons Inc., 1999.
- [26] S. Afrasiabi-Gorgani and G. Wunder, "The Method of Conditional Expectations for Cubic Metric Reduction in OFDM," in *2019 IEEE 20th International Workshop on Signal Processing Advances in Wireless Communications (SPAWC)*, July 2019, pp. 1–5.
- [27] W. Rudin, *Real and Complex Analysis, 3rd Ed*. New York, NY, USA: McGraw-Hill, Inc., 1987.
- [28] M. R. Leadbetter and H. Rootzen, "Extremal theory for stochastic processes," *Ann. Probab.*, vol. 16, no. 2, pp. 431–478, 04 1988. [Online]. Available: <https://doi.org/10.1214/aop/1176991767>
- [29] S. Wei, D. L. Goeckel, and P. E. Kelly, "A modern extreme value theory approach to calculating the distribution of the peak-to-average power ratio in OFDM systems," in *2002 IEEE International Conference on Communications. Conference Proceedings. ICC 2002 (Cat. No.02CH37333)*, vol. 3, 2002, pp. 1686–1690 vol.3.